Mathematical modeling predicts response to chemotherapy and drug combinations in ovarian cancer

Emilia Kozłowska[1], Anniina Färkkilä[2], Tuulia Vallius[3], Olli Carpén[1,4], Jukka Kemppainen[5], Seija Grénman[3], Rainer Lehtonen[1], Johanna Hynninen[3], Sakari Hietanen[3], Sampsa Hautaniemi[1,*]

[1]Genome-Scale Biology Research Program, Research Programs Unit, Faculty of Medicine, University of Helsinki, Finland; [2]Department of Radiation Oncology, Dana-Farber Cancer Institute, Harvard Medical School, USA; [3]Department of Obstetrics and Gynecology, Turku University Hospital, University of Turku, Finland; [4]Department Pathology, Turku University Hospital, University of Turku, Finland; [5]Department of Clinical Physiology and Nuclear Medicine, Turku University Hospital, University of Turku, Finland

Abstract

Platinum-based chemotherapy constitutes the backbone of clinical care in advanced solid cancers such as high-grade serous ovarian cancer (HGSOC) and has prolonged survival of millions of cancer patients. Most of these patients, however, become resistant to chemotherapy, which generally leads to a fatal refractory disease. We present a comprehensive stochastic mathematical model and simulator approach to describe platinum resistance and standard-of-care (SOC) therapy in HGSOC. We used pre- and post-treatment clinical data, including 18F-FDG-PET/CT images, to reliably estimate the model parameters and simulate "virtual HGSOC patients." Treatment responses of the virtual patients generated by our mathematical model were indistinguishable from real-life HGSOC patients. We demonstrated the utility of our approach by evaluating the survival benefit of combination therapies that contain up to six drugs targeting platinum resistance mechanisms. Several resistance mechanisms were already active at diagnosis, but combining SOC with a drug that targets the most dominant resistance subpopulation resulted in a significant survival benefit. This work provides a theoretical basis for a cancer treatment paradigm in which maximizing platinum's killing effect on cancer cells requires overcoming resistance mechanisms with targeted drugs. This freely available mathematical model and simulation framework enable rapid and rigorous evaluation of the benefit of a targeted drug or combination therapy in virtual patients before clinical trials, which facilitates translating preclinical findings into clinical practice.

Introduction

Platinum-based chemotherapy constitutes the backbone of clinical care in advanced solid cancers. Cisplatin, and its less toxic analogs, carboplatin, oxaliplatin, and nedaplatin, have been used for more than 40 years in most solid cancers, including metastatic colorectal (1), triple-negative breast (2), and prostate (3) cancers. Platinum is curative in testicular cancers (4); in epithelial ovarian cancer it has improved the 10-year survival rate by over 10% and more than doubled the number of complete responses (5,6). While platinum-based chemotherapy has prolonged the survival of millions of patients, majority of them still develop resistance, which usually leads to a refractory disease with very short life expectancy.

We focus herein on high-grade serous ovarian cancer (HGSOC), which is the most common epithelial ovarian cancer subtype and accounts for 70-80% of ovarian cancer deaths (7,8). The

first-line standard-of-care (SOC) therapy for HGSOC consists of a cytoreductive surgery, followed by platinum-based chemotherapy (8). In a recent guideline, the Society of Gynecologic Oncology and the American Society of Clinical Oncology recommends that patients with a high perioperative risk profile or a low likelihood to obtain optimal cytoreduction should receive neoadjuvant chemotherapy (NACT) before surgery and adjuvant chemotherapy (8). In a majority of patients, NACT reduces tumor burden significantly, as shown in Figure 1. However, even though 90% of the HGSOC patients show no clinically detectable signs of cancer after surgery and chemotherapy, the five-year survival rate in HGSOC is still less than 50%, making epithelial ovarian cancer the fifth leading cause of female cancer deaths worldwide (9,10).

HGSOC tumors are characterized by high intra-tumoral heterogeneity (11), which leads to cancer cell subpopulations with various platinum resistance mechanisms. Resistance mechanisms can exist in a subpopulation already at diagnosis (intrinsic resistance) or develop in a previously sensitive cancer cell due to chemotherapy (acquired resistance). Here we focus on intrinsic resistance, which is suggested to be the dominant resistance model in HGSOC by evolutionary studies (12,13). Several platinum resistance related processes have been identified, including reduced intake or increased efflux or platinum, DNA repair mechanisms, xenobiotics pathways and dysfunctional apoptosis machinery (7,14,15). However, it is still unclear how many of them are active already at diagnosis even though the number of active resistance mechanisms at diagnosis and after chemotherapy has direct implications to planning treatment regimens.

Several drugs that are approved for cancer care could be used in combination with the current SOC to increase survival rates in HGSOC. However, establishing the benefit of a drug or a combination therapy over SOC in clinical trials is expensive and slow. We introduce here a stochastic mathematical model for chemotherapy resistance in HGSOC and use it to create "virtual HGSOC patients." These virtual patients can be used to estimate the number of active resistance mechanisms at diagnosis or after treatment and to suggest guidelines for developing effective combination therapy regimens.

Our approach takes advantage of rich clinical data, including ^{18}F-fluorodeoxyglucose positron emission tomography/computed tomography (^{18}F-FDG-PET/CT) imaging. Cancer cells with low proliferation rate have low ^{18}F-FDG uptake and are associated with a less aggressive disease, whereas high ^{18}F-FDG uptake is associated with a more aggressive disease. Thus, ^{18}F-FDG-PET/CT allows accurate estimates of total metabolic tumor burden, collected before and after chemotherapy (Figure 1A). Our results indicate that the virtual cancer patients have indistinguishable treatment responses from real-life patients. Thus, the benefit of a targeted drug or combination therapy over SOC can be evaluated rapidly and rigorously with our approach. This facilitates translating preclinical findings efficiently into clinical trials and, eventually, patient care.

Materials and Methods

Clinical characteristics of the calibration and validation cohorts

Clinical data were collected prospectively from 62 patients treated for ovarian or primary peritoneal HGSOC at Turku University Hospital from Oct 2009 to July 2016 (Table 1, Supplementary Table 1). All the calibration cohort patients had been evaluated as inoperable in the diagnostic laparoscopy and were referred to NACT treatment before surgery. NACT consisted of median three (range 1-5) cycles of carboplatin and paclitaxel chemotherapy. For

patients who responded to NACT, an interval debulking surgery (IDS) was performed, aiming for optimal cytoreduction, followed by a median of three (range 0-9) cycles of adjuvant chemotherapy.

Residual disease was reported based on the surgeon's visual estimation of the amount of macroscopic tumor left after IDS. The primary therapy response was defined according to RECIST 1.1 criteria (16). Twenty-eight (45%) patients had complete response, 13 (21%) had partial response, 20 (32%) patients had progressive disease, and one patient died during primary therapy and thus the response could not be evaluated. All patients participating in the study gave written informed consent. The study and the use of all clinical material have been approved by (i) The Ethics Committee of the Hospital District of Southwest Finland (ETMK): ETMK 53/180/2009 § 238 and (ii) National Supervisory Authority for Welfare and Health (Valvira): DNRO 6550/05.01.00.06/2010 and STH507A.

We used The Cancer Genome Atlas (TCGA) data as an independent validation cohort (clinical data downloaded from the TCGA data portal in December 2016) (17). The TCGA cohort consists of 489 patients with clinical data. Patient selection criteria for the validation cohort were as follows: 1) advanced high-grade serous ovarian cancer (grade>1, stage: IIIb-IV), 2) an indication of attempted surgical debulking, *i.e.*, information available on the residual disease, and 3) treatment by platinum-based chemotherapy alone or in combination in the first-line setting. In order to conform to current therapy standards, we did not exclude patients who received bevacizumab, an angiogenesis inhibitor, which has been shown to improve progression-free survival in HGSOC (18), as a maintenance therapy. After applying these selection criteria, the validation cohort consisted of 170 HGSOC patients.

The patient characteristics of the calibration and validation cohorts are summarized in Table 1. The patients in the calibration cohort were older, had more often advanced stage (IV) disease, and received more often single platinum therapy and bevacizumab maintenance after the first-line treatment. The patients in the calibration cohort also had less residual disease after debulking surgery compared to the validation cohort. There were more patients with progressive disease in the calibration cohort, and progression-free survival was shorter in the validation cohort. However, there were no significant differences in therapy responses, *i.e.*, platinum-free interval or progression free/overall survival, between the cohorts.

Tumor burden estimation with ^{18}F-FDG-PET/CT

For 28 patients in our calibration cohort, ^{18}F-fluorodeoxyglucose positron emission tomography/computed tomography (^{18}F-FDG-PET/CT) imaging was performed at the time of diagnosis and after NACT, as described in (19). The ^{18}F-FDG-PET/CT images were used to evaluate the total metabolic tumor volume (MTV) before and after NACT. Two patients did not have visible residual tumor in PET/CT images after NACT and were excluded from further analysis as their tumor burden could not be evaluated.

The total tumor burden was estimated using the metabolic tumor volume (MTV), which is defined as the sum volume of all the tumor lesions with increased ^{18}F-FDG uptake. The MTV calculations were done by expert nuclear medicine physician as follows. The PET images were reconstructed in 3D mode and 128 x 128 matrix size using the ML-OSEM reconstruction algorithm. Imaging analysis was performed using ADW 4.6 workstation (General Electric Medical Systems, Milwaukee, WI, USA). The metabolically active lesions were identified semi-automatically with PET VCAR (Volume Computer Assisted Reading) program by comparing the pre- and post-NACT ^{18}F-FDG-PET/CT images. All the suggested lesions with

increased ^{18}F-FDG uptake were either bookmarked as a tumor lesion or removed in cases of physiological uptake, such as ureters and bladder.

Mathematical model to describe HGSOC patient responses to chemotherapy and surgery
We applied a stochastic multitype branching process (20) to model tumor growth and evolution. Briefly, our model describes clonal expansion of cancer cells starting from a single platinum-sensitive cell that can divide at rate b and die at rate d, giving the net growth rate $\lambda = b-d$. A cell can acquire resistance mechanisms at rate u per cell division independent of chemotherapy. Resistance accumulates sequentially, *i.e.*, a cell with n active resistance mechanism can accumulate n+1 resistance mechanisms that are irreversible. The schematic of the model is given in Figure 2A and in more detail in Supplementary Text 1-3.

The integration of clinical data and modeling is outlined in Figure 2B. We estimated the key model parameters using our calibration cohort, and the values for other parameters were collected from previous studies (21–23). All model parameters together with their values are listed in Table 2. Details of the parameter calibration are provided in Supplementary Text 4.

Creation of a virtual HGSOC cohort
We used the stochastic mathematical model and simulation approach to create a virtual HGSOC patient cohort that has similar responses to chemotherapy as observed in the real-life HGSOC cohort. Briefly, for each virtual patient, the values of tumor burden at diagnosis (M) and chemotherapy effect ($d_{chemotherapy}$) were sampled from log-normal distributions while the other parameters were kept constant, as shown in Table 2. The log-normal distribution was the best match to describe the data among six statistical distributions using Bayesian Information Criterion (Supplementary Material S4). All virtual patients were simulated until tumor relapse, *i.e.*, to the point where the total number of cancer cells reaches $M_{relapse}$ cells.

In the simulations, the effect of a drug is measured by platinum-free interval (PFI), which is the interval from the last date of chemotherapy until progression (24). PFI is used in clinical practice to measure a patient's sensitivity to platinum and to group them into platinum-sensitive, -resistant, and refractory, and to guide treatment decisions (14,25,26).

Results

Mathematical model captures treatment responses to SOC
We have constructed a stochastic multitype branching process mathematical model that describes chemotherapy sensitive and resistant cell growth in HGSOC (Figure 2A). A stochastic model allows modeling an arbitrary number of resistant mechanisms and thus our analyses are not limited by the number of resistance mechanisms.

Figure 2B shows how clinical data was integrated into the model, and the standard-of-care (SOC) simulation is described in Figure 2C. Briefly, during the pre-diagnosis phase the tumor burden increases without intervention. After the diagnosis, the treatment phase starts with NACT, followed by cytoreductive surgery and adjuvant chemotherapy. The post-treatment phase continues until a relapse is detected. Detailed descriptions of the model structure and major assumptions are given in Methods and Supplementary Text S1.

To quantify the effect of chemotherapy, we measured both tumor burden and platinum-free interval (PFI) and used them to create a virtual HGSOC cohort of 1,000 patients (see Methods). The ratio of the standard deviation to the mean tumor burden was 0.46 before NACT and 1.15 after NACT in the calibration cohort, which indicates high individual variation in response to

chemotherapy. Response variation in the virtual HGSOC cohort is indistinguishable from the real-life calibration cohort (Kolmogorov-Smirnov test $p>0.05$; Supplementary Figure S1). Median PFI of patients in the virtual HGSOC cohort is seven months, which is in line with the median PFI in the calibration cohort (five months) and is identical to the validation cohort, as shown in Figure 3A. These results show that the clinically important characteristics of treatment responses, *i.e.*, individual variation and PFI, of real-life HGSOC patients are faithfully reproduced by the mathematical model.

Sensitivity analysis shows that surgery and tumor aggressiveness have the largest effect to PFI

To identify the most influential parameters in the model, we conducted a sensitivity analysis. Briefly, sensitivity analysis quantitatively ranks the strength of the relationship between all model parameters (Table 2) and platinum-free survival (Supplementary Text 5). We considered a parameter sensitive if the sensitivity coefficient (SC), which measures the ratio of the change in the output (area under survival curve) to the change in input, is at least 50%.

The parameters which had high sensitivity, and therefore a high impact on the PFI, were the fraction of cells removed in surgery (β), death rate (d), and division rate (b), as illustrated in Figure 3B. The death and division rates reflect the inherent growth pattern and aggressiveness of a tumor. Thus, their ranking as sensitive parameters was expected. The impact of interval debulking surgery on PFI is supported by several clinical trials which have demonstrated that optimal cytoreduction yields a significant survival benefit (27,28).

Interestingly, tumor burden at diagnosis (M) did not have a large effect on PFI (sensitivity coefficient -12%). This is in accordance with the training cohort, in which the tumor burden at diagnosis did not correlate well with response to NACT (Pearson correlation coefficient 0.17). The modest effect of tumor burden at diagnosis on PFI suggests that earlier detection of HGSOC will only lead to a relatively modest survival benefits. Our results thus further corroborate previous modeling efforts which concluded that detection of HGSOC with small tumor volume does not significantly improve response to therapy (29,30).

Platinum therapy changes the number and proportion of active resistant mechanisms

Given the significant effect of tumor aggressiveness on PFI, we next explored the number of active resistance mechanisms present in HGSOC tumors at the time of diagnosis by using the virtual cohort of 1,000 patients. In addition to the number of active resistance mechanisms, we also investigated the proportion of resistance mechanisms in tumors before and after NACT.

At diagnosis, majority of patients (55%) had tumors that contained cancer cells with five active resistant mechanisms, and their average PFI was six months. Forty percent of the patients had four active resistance mechanisms and an average PFI of ten months, while 5% of the HGSOC patients had six active mechanisms and an average PFI of six months. The fraction of resistant cells at diagnosis had a high correlation with PFI (Pearson correlation coefficient 0.60). Notably, 83% of the cancer cells were platinum sensitive at diagnosis, and only 1% of the cells had three or more active resistance mechanisms (Figure 4A), which is consistent with the clinical efficacy of platinum on reducing tumor burden in HGSOC.

An average virtual HGSOC patient had approximately 10^7 cancer cells after NACT. Of all the cancer cells that survived NACT, the fraction of platinum sensitive cells was dramatically reduced to 11% (Figure 4B), which suggests limited efficiency of the subsequent platinum-based chemotherapy cycles. However, 99% of the cancer cells that survived NACT had at most

two active resistant mechanisms (Figure 4B). This implies that the vast majority of the cancer cells removed at IDS are platinum resistant, but combining targeted therapies to the adjuvant chemotherapy regimens after NACT and IDS could provide a significant survival benefit.

Virtual patient cohorts enable the evaluation of the added value of combination treatments

We next investigated the benefit of combining targeted therapies to SOC. High proportion of cancer cells with less than four active resistance mechanisms even after chemotherapy suggests that combining SOC with only a few additional drugs should improve to patient survival significantly. We tested this hypothesis by simulating up to six targeted therapies in combination with SOC in the virtual patient cohort.

We calculated PFI estimates for SOC alone and for regimens where SOC was combined with at most six drugs targeting resistance mechanisms. The PFIs for the combination therapies are shown in Figure 5. The median PFI for SOC was 7 months, and adding only one effective targeted therapy to SOC increased the median PFI to 25 months. The addition of more targeted drugs to SOC improved the PFI, but relatively less than the first drug. For example, addition of a second effective targeted therapy to the regimen improved the median PFI to 45 months and a third targeted therapy improved the median PFI to 60 months. Adding a fourth, fifth or sixth drug did not bring any significant benefit over combining three targeted therapies with SOC.

Discussion

Resistance to chemotherapies is the major contributor to cancer-related mortality, and a deeper understanding of the prevalence and dynamics of active resistance mechanisms is needed to improve patient survival. HGSOC is typically diagnosed at an advanced stage with significant innate heterogeneity and, likely, several active resistance mechanisms already at diagnosis. Indeed, only few targeted agents with encouraging preclinical results in HGSOC have converged into significant clinical responses, and the survival rate of HGSOC patients has not markedly improved over the past 30 years. We propose here that mathematical modeling and simulation using rich clinical data offers a means to reliably evaluate the value of preclinical agents in virtual cohorts. This approach allows testing the added value of combination therapies, which may be difficult or expensive to test *in vivo* or in patients, in an efficient and inexpensive manner, as previously suggested by us and others (31–33).

Our approach takes advantage of the accumulated knowledge of rich longitudinal clinical data from HGSOC patients. In particular, the values of key parameters in the model, such as tumor burden and the effect of chemotherapy, were quantified with ^{18}F-FDG-PET/CT, which is an order of magnitude times more sensitive than a contrast-enhanced CT scan. This allowed creating virtual HGSOC patients whose responses to SOC are indistinguishable from real-life HGSOC patients.

Approximately 30% of HGSOC patients are platinum refractory already at diagnosis, and most patients initially responding to platinum will develop a platinum resistant relapse. These patients with advanced platinum resistant disease have currently very limited treatment options (8). Therefore, we focused on this patient population to uncover the active resistance mechanisms and the value of targeted therapies. All patients in the calibration cohort had been clinically assigned to receive NACT due to advanced and disseminated disease, whereas majority of patients in the validation cohort were treated with primary debulking surgery followed by adjuvant chemotherapy, indicating a less advanced disease at diagnosis. Therefore, the observed good fit to patient responses in both cohorts provides strong validation that the

model is able to accurately simulate clinical outcome after first-line SOC in a clinically heterogeneous HGSOC patient population treated with or without NACT.

Sensitivity analysis indicated that the most important parameter was the fraction of cells removed in the surgery. Debulking surgery is a very effective strategy to reduce tumor burden and, unlike chemotherapy, it can remove a significant portion of chemotherapy resistant cells, which reduces the probability of resistance (34). Importance of surgery is supported by clinical trials demonstrating that optimal cytoreduction yields a significant survival benefit (27,28). Perhaps unexpectedly, platinum efficacy had only a small impact to PFI. This is due to the fact that while chemotherapy effectively kills drug sensitive cancer cells, it also provides a selective advantage for resistant cells that can grow with less constraints on space and nutrients. A higher fraction of resistant cells rapidly reduces PFI in the subsequent chemotherapy cycles, leading to refractory disease and death. Thus, development of platinum compounds with higher efficacy may have a limited impact to HGSOC patient survival.

Combination therapy has been suggested as an effective means to overcome therapy failures in advanced solid cancers (35). It is, however, not generally known how many drugs should be combined to achieve a significant and long-lasting survival advantage. Our results indicate that at diagnosis there are already up to five resistance mechanisms active in a fraction of the tumor cells. However, before chemotherapy platinum sensitive cells form 80% of the cancer cell population, which explains the generally observed good response to chemotherapy in HGSOC. Importantly, after neoadjuvant chemotherapy, the proportion of chemosensitive cells is reduced to 11%, and 88% of the cancer cells now have only one or two active resistance mechanisms. This provides a window of opportunity to target the dominant resistant subpopulations with few targeted drugs and potentially gain significant survival benefit. Our results also suggest that combining four or more targeted therapies to SOC has a marginal effect on patient survival over three drugs. This is due to a small proportion of cancer cells having four of more active resistance mechanisms.

Throughout our analyses we have assumed that a targeted therapy kills those cancer cells that contain the respective active resistance mechanism as efficiently as platinum kills platinum sensitive cancer cells. However, the efficacy of each therapy may vary, and the combination treatments may present synergistic effects (36). We also assumed that targeted therapies are given at tolerated doses in combination with SOC. However, the targeted agents may have significant overlapping toxicities, which need to be modeled for each specific targeted therapy using pharmacological data. Importantly, these biological and clinical factors can be implemented into our model to further improve its clinical value.

Our results provide a theoretical basis for a treatment paradigm where the objective is to maximize platinum's effect on cancer cells by simultaneously overcoming resistance mechanisms with targeted drugs. For this approach, it is crucial to have reliable biomarkers to identify the most dominant resistance mechanisms in tumors before the treatment. Furthermore, our results show that the fraction of the resistance mechanisms significantly changes during the treatment, which suggests that the development and use of serial sampling is needed in planning secondary or maintenance treatments.

The herein presented mathematical model has been developed using clinical data from HGSOC patients. It is, however, straightforward to modify the model and parameters to accommodate other cancers and therapy regimens. The mathematical model and simulator are available with comprehensive documentation at http://csbi.ltdk.helsinki.fi/pub/home/ekozlows/platinum/ .

Acknowledgements

We thank Dr. Krzysztof Puszyński for critical review of the manuscript, MSc Tiia Pelkonen for proof-reading, and CSC – IT Center for Science Ltd. for compute resources. This project has received funding from the European Union's Horizon 2020 research and innovation program under grant agreement No 66740, the Academy of Finland, the Sigrid Jusélius Foundation, and Finnish Cancer Associations. The results published here are in part based upon data generated by The Cancer Genome Atlas managed by the NCI and NHGRI. Information about TCGA can be found at http://cancergenome.nih.gov.

References

1. Chibaudel B, Tournigand C, Bonnetain F, Maindrault-Goebel F, Lledo G, André T, et al. Platinum-sensitivity in metastatic colorectal cancer: Towards a definition. Eur J Cancer. 2013;49:3813–20.

2. Isakoff SJ, Mayer EL, He L, Traina TA, Carey LA, Krag KJ, et al. TBCRC009: A multicenter phase II clinical trial of platinum monotherapy with biomarker assessment in metastatic triple-negative breast cancer. J Clin Oncol. 2015;33:1902–9.

3. Aparicio AM, Harzstark AL, Corn PG, Wen S, Araujo JC, Tu SM, et al. Platinum-based chemotherapy for variant castrate-resistant prostate cancer. Clin Cancer Res. 2013;19:3621–30.

4. Kelland L. The resurgence of platinum-based cancer chemotherapy. Nat Rev Cancer. 2007;7:573–84.

5. Neijt JP, ten Bokkel Huinink WW, van der Burg MEL, van Oosterom AT, Willemse PHB, Vermorken JB, et al. Long-term survival in ovarian cancer. Eur J Cancer Clin Oncol. 1991;27:1367–72.

6. Cristea M, Han E, Salmon L, Morgan RJ. Practical considerations in ovarian cancer chemotherapy. Ther Adv Med Oncol. 2010;2:175–87.

7. Bowtell DD, Böhm S, Ahmed A a, Aspuria P-J, Bast RC, Beral V, et al. Rethinking ovarian cancer II: reducing mortality from high-grade serous ovarian cancer. Nat Rev Cancer. Nature Publishing Group; 2015;15:668–79.

8. Wright AA, Bohlke K, Armstrong DK, Bookman MA, Cliby WA, Coleman RL, et al. Neoadjuvant chemotherapy for newly diagnosed, advanced ovarian cancer: Society of Gynecologic Oncology and American Society of Clinical Oncology Clinical Practice Guideline. J Clin Oncol. 2016;34:3460–73.

9. Siegel R, Miller K, Jemal A. Cancer statistics , 2015 . CA Cancer J Clin. 2015;65:29.

10. Vergote I, Tropé CG, Amant F, Kristensen GB, Ehlen T, Johnson N, et al. Neoadjuvant chemotherapy or primary surgery in stage IIIC or IV ovarian cancer. N Engl J Med. Massachusetts Medical Society; 2010;363:943–53.

11. Schwarz RF, Ng CKY, Cooke SL, Newman S, Temple J, Piskorz AM, et al. Spatial and temporal heterogeneity in high-grade serous ovarian cancer: a phylogenetic analysis. PLoS Med. 2015;12:e1001789.

12. Cooke SL, Ng CKY, Melnyk N, Garcia MJ, Hardcastle T, Temple J, et al. Genomic analysis of genetic heterogeneity and evolution in high-grade serous ovarian carcinoma. Oncogene. 2010;29:4905–13.

13. Castellarin M, Milne K, Zeng T, Tse K, Mayo M, Zhao Y, et al. Clonal evolution of high-grade serous ovarian carcinoma from primary to recurrent disease. J Pathol. 2013;229:515–24.

14. Galluzzi L, Senovilla L, Vitale I, Michels J, Martins I, Kepp O, et al. Molecular mechanisms of cisplatin resistance. Oncogene. Nature Publishing Group; 2012;31:1869–83.

15. Bookman M a. First-line chemotherapy in epithelial ovarian cancer. Clin Obstet Gynecol. 2012;55:96–113.

16. Eisenhauer EA, Therasse P, Bogaerts J, Schwartz LH, Sargent D, Ford R, et al. New response evaluation criteria in solid tumours: Revised RECIST guideline (version 1.1). Eur J Cancer. Elsevier Ltd; 2009;45:228–47.

17. Bell D, Berchuck A, Birrer M, Chien J, Cramer DW, Dao F, et al. Integrated genomic analyses of ovarian carcinoma. Nature. 2011;474:609–15.

18. Lai GGY, Penson RT. Bevacizumab and ovarian cancer. Drugs of Today. 2011;47:669–81.

19. Vallius T, Hynninen J, Kemppainen J, Alves V, Auranen K, Matomäki J, et al. 18F-FDG-PET/CT based total metabolic tumor volume change during neoadjuvant chemotherapy predicts outcome in advanced epithelial ovarian cancer. Eur J Nucl Med Mol Imaging. European Journal of Nuclear Medicine and Molecular Imaging; 2018;c.

20. Durrett R. Branching process models of cancer. Branch. Process Model. Cancer. Cham: Springer International Publishing; 2015.

21. Panetta JC. A mathematical model of breast and ovarian cancer treated with paclitaxel. Math Biosci. 1997;146:89–113.

22. Brown PO, Palmer C. The preclinical natural history of serous ovarian cancer: Defining the target for early detection. PLoS Med. 2009;6:e1000114.

23. Del Monte U. Does the cell number 109 still really fit one gram of tumor tissue? Cell Cycle. 2009;8:505–6.

24. Friedlander M, Trimble E, Tinker A, Alberts D, Avall-Lundqvist E, Brady M, et al. Clinical Trials in Recurrent Ovarian Cancer. Int J Gynecol Cancer. 2011;21:771–5.

25. Davis A, Tinker A V., Friedlander M. "platinum resistant" ovarian cancer: What is it, who to treat and how to measure benefit? Gynecol Oncol. Elsevier B.V.; 2014;133:624–31.

26. Galluzzi L, Vitale I, Michels J, Brenner C, Szabadkai G, Harel-Bellan A, et al. Systems biology of cisplatin resistance: past, present and future. Cell Death Dis. Nature Publishing Group; 2014;5:e1257.

27. Polterauer S, Vergote I, Concin N, Braicu I, Chekerov R, Mahner S, et al. Prognostic value of residual tumor size in patients with epithelial ovarian cancer FIGO stages IIA–IV. Int J Gynecol Cancer. 2012;22:380–5.

28. Winter WE, Maxwell GL, Tian C, Sundborg MJ, Rose GS, Rose PG, et al. Tumor residual after surgical cytoreduction in prediction of clinical outcome in stage IV epithelial ovarian cancer: A Gynecologic Oncology Group study. J Clin Oncol. 2008;26:83–9.

29. Danesh K, Durrett R, Havrilesky LJ, Myers E. A branching process model of ovarian cancer. J Theor Biol. 2012;314:10–5.

30. Botesteanu D, Lee J, Levy D, Lipkowitz S, Lee J, Levy D. Modeling the Dynamics of High-Grade Serous Ovarian Cancer Progression for Transvaginal Ultrasound-Based Screening and Early Detection. PLoS One. 2016;11:e0156661.

31. Hua F, Hautaniemi S, Yokoo R, Lauffenburger DA. Integrated mechanistic and data-driven modelling for multivariate analysis of signalling pathways. J R Soc Interface. 2006;3:515–26.

32. Hautaniemi S, Kharait S, Iwabu A, Wells A, Lauffenburger DA. Modeling of signal-response cascades using decision tree analysis. Bioinformatics. 2005;21:2027–35.

33. Kim E, Rebecca VW, Smalley KSM, Anderson ARA. Phase i trials in melanoma: A framework to translate preclinical findings to the clinic. Eur J Cancer. 2016;67:213–22.

34. Fagotti A, Gallotta V, Romano F, Fanfani F, Rossitto C, Naldini A, et al. Peritoneal carcinosis of ovarian origin. World J Gastrointest Oncol. 2010;2:102–8.

35. Bozic I, Reiter JG, Allen B, Antal T, Chatterjee K, Shah P, et al. Evolutionary dynamics of cancer in response to targeted combination therapy. Elife. 2013;2013:1–15.

36. Palmer AC, Sorger PK. Combination Cancer Therapy Can Confer Benefit via Patient-to-Patient Variability without Drug Additivity or Synergy. Cell. Elsevier Inc.; 2017;171:1678–1682.e13.

Tables

Characteristic	Cohort		
	Calibration n=62	**TCGA n=170**	**p-value for difference**
Age at diagnosis (years)	66 (38-83)	59 (30-87)	<0.0001[4]
Tumor stage (FIGO 2009)			
IIIB	1 (2)	9 (5)	0.0009[5]
IIIC	37 (60)	134 (79)	
IV	24 (39)	27 (16)	
MTV (cm^3)			
Before NACT	345 (150 – 787)	NA	NA
After NACT	47 (0 – 417)		
Residual tumor after DS			
0	14 (23)	26 (15)	<0.0001[5]
1 to 10mm	27 (44)	87 (51)	
>10mm	4 (7)	57 (34)	
NA	16 (26)	0	
Primary chemotherapy regimens			
Platinum[1]	9 (15)	7 (4)	0.02[5]
Platinum – Taxane[2]	53 (85)	163 (96)	
Bevacizumab maintenance			
Yes	14 (22)	5 (3)	<0.0001[5]
No	48 (78)	165 (97)	
Primary therapy outcome			
Complete response	28 (45)	115 (68)	<0.0001[5]
Partial response	13 (21)	25 (15)	
Stable disease	0	8 (5)	
Progressive disease	20 (32)	9 (5)	
NA	1	13 (8)	
Platinum-free interval (months)	5 (0 – 22)	7(0 - 108)	0.01[6]
Progression-free survival (months)[3]	10 (1 – 27)	13 (3 – 113)	<0.0001[6]
Overall survival (months)	18 (2 – 65)	37 (3 – 154)	<0.0001[6]

Table 1. Summary of the patient cohorts. The data are presented as median (range), or N (%), MTV = Metabolic Tumor Volume, DS = Debulking surgery. [1]carboplatin or cisplatin, [2]paclitaxel or docetaxel combined with platinum, [3]Time from diagnosis to progression. [4]Student's t-test, [5]Fisher's Exact Test, [6]Mann-Whitney-U test.

Symbol	Value	Unit	Description	Reference
b	0.667	$\frac{1}{\text{day}}$	Division rate	Taken from (21)
d	0.661	$\frac{1}{\text{day}}$	Death rate	Taken from (22)
u	$1.6 \cdot 10^{-5}$	$\frac{1}{\text{cell division}}$	Transition rate	Estimated from calibration cohort clinical data
M	$3.959 \cdot 10^{11}$	# of cells	Tumor burden at diagnosis	Computed from the PET/CT imaging data
$M_{relapse}$	10^9	# of cells	Tumor burden at recurrence	Taken from (23)
$d_{chemotherapy}$	0.33	–	Chemotherapy effects on sensitive cells	Computed from the PET/CT imaging data
β	2	cell-log kill	Fraction of cells removed by surgery	Computed from the calibration cohort clinical data

Table 2. Parameters and their values in the mathematical model. "–" represents a dimensionless unit.

Figures

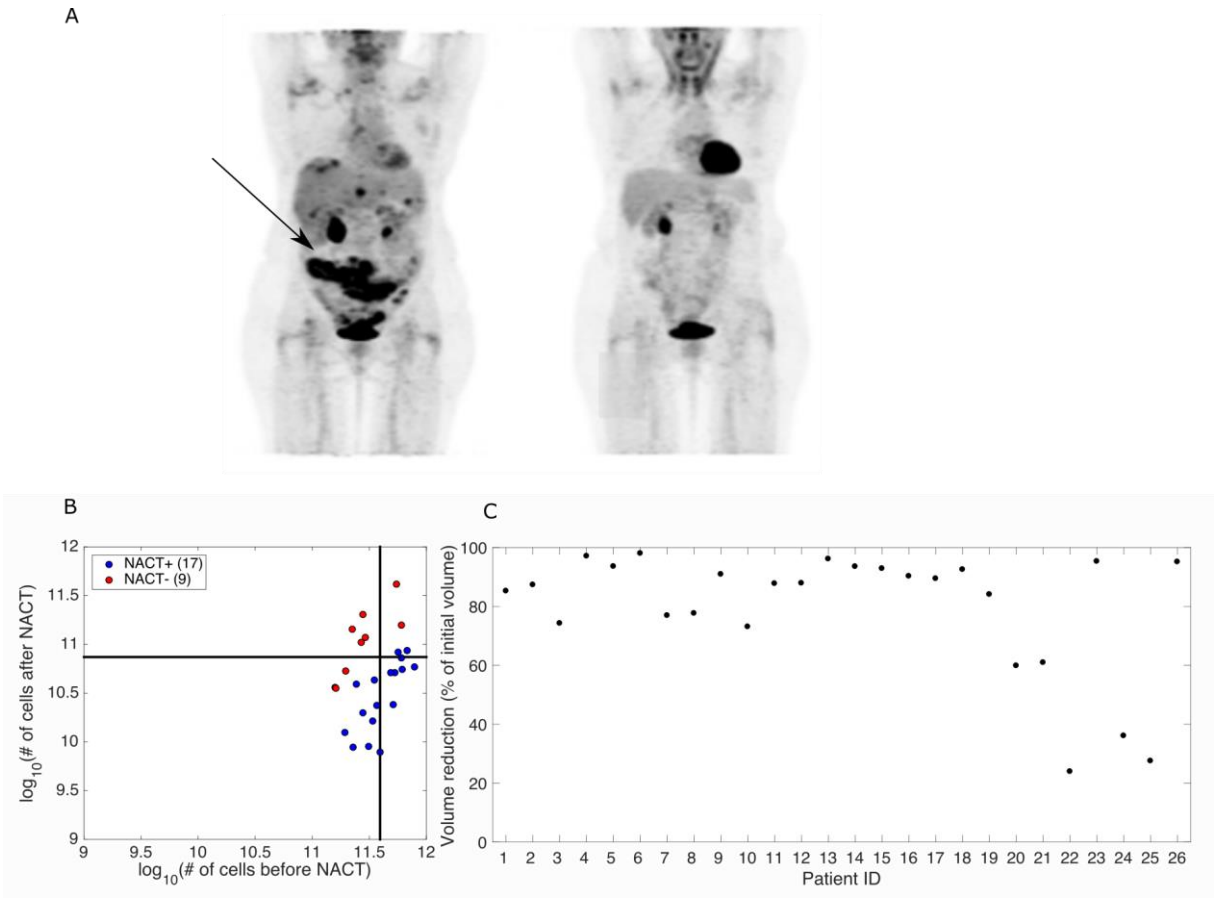

Figure 1: The effect of neoadjuvant chemotherapy (NACT) on tumor burden. Panel A. Illustration of an average decrease in total metabolic tumor volume during NACT. Patient #19 underwent ^{18}F-FDG-PET/CT before (left) and after (right) NACT. Tumor tissue is marked with an arrow. A reduction of 80% in total MTV during NACT was observed. **Panel B**. At diagnosis, the average tumor burden of an HGSOC patient in the calibration cohort is 393 cm^3 ($3.9 \cdot 10^{11}$ tumor cells). After NACT, the average tumor burden has decreased to 74 cm^3 ($7.4 \cdot 10^{10}$ tumor cells). Approximately 70% of the patients have at least 80% decrease in tumor burden (marked as NACT+). **Panel C**. NACT provides a large tumor burden reduction in average, but there are large differences in the efficacy of chemotherapy on tumor burden between individual patients. The coefficient of variation for tumor burden (defined as the ratio of the standard deviation to the mean) before and after NACT was 0.46 and 1.15, respectively.

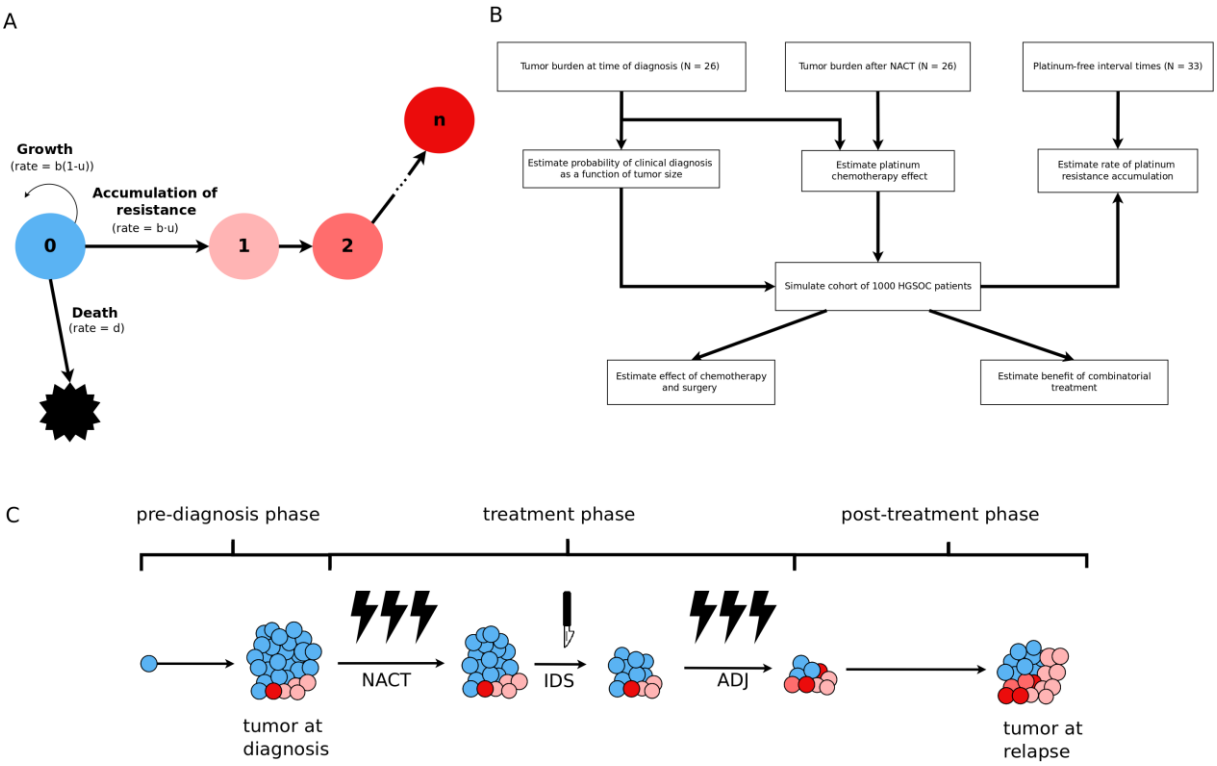

Figure 2: Schematics of the mathematical model and treatment simulation. Panel A. Resistance to platinum in HGSOC is modeled as a stochastic multitype birth-death-mutation process. Tumor development starts from a single platinum-sensitive cell that divides with rate *b(1-u)* and dies with rate *d*. In addition, cancer cells can accumulate additional resistance mechanism with rate $b \cdot u$. We assume a gradual model of resistance evolution, where the cell with a given number of resistance mechanisms can gain one additional resistance mechanism. Parameter *b* is birth rate, *u* is transition rate and *d* is death rate. **Panel B**. Schematic of our modeling strategy. Estimated tumor burden at diagnosis and after three cycles of NACT from 26 patients was applied to estimate the value of tumor burden at diagnosis (*M*) and the effect of chemotherapy on sensitive cells ($d_{chemotherapy}$). In addition, a measure of response to platinum (platinum-free interval) was applied to estimate the value of transition rate (*u*). **Panel C**. Schematic of SOC in HGSOC simulation. Cancer is diagnosed when the tumor burden reaches *M* cells. Primary treatment phase starts after diagnosis and consists of neoadjuvant chemotherapy, debulking surgery, and adjuvant chemotherapy. Chemotherapy is modeled by increasing the death rate of sensitive cells proportionally to the division rate. Surgery is modeled as instantaneous removal of a fraction of tumor cells. Full description of the model and simulation is available in supplementary material. NACT = Neoadjuvant chemotherapy; IDS = Interval debulking surgery; ADJ = Adjuvant chemotherapy.

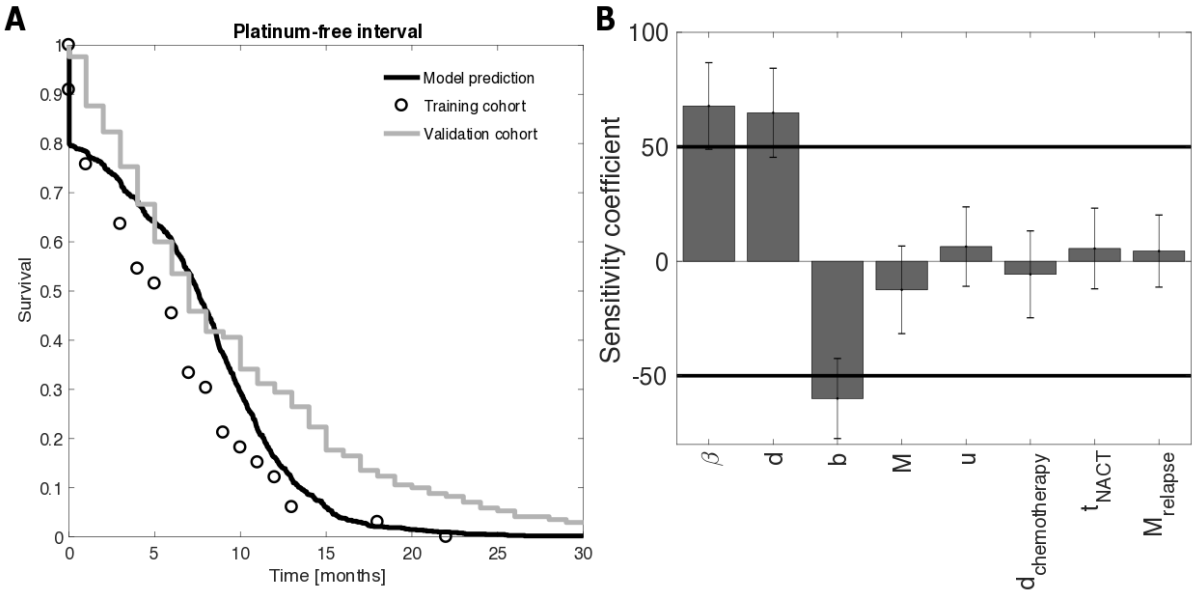

Figure 3: Matching model predictions with calibration and validation cohorts. Panel A. Estimates of platinum free interval (PFI) for the calibration cohort, validation cohort and model predictions are plotted as a function of time. To evaluate the goodness-of-fit between the observed and the predicted platinum free survival plots, we applied two different statistical methods: Mean Squared Error (MSE), and two-sample Kolmogorov-Smirnov test. The minimum of MSE is 0.09 for the parameter values listed in Table 2. The two-sample Kolmogorov-Smirnov test did not reject the null hypothesis that all predictions using estimated parameters and experimental data are from the same distribution ($p > 0.05$). The ability to simulate HGSOC patient responses that are very close to real-life cohorts allows accurate evaluation of the benefit of combination treatments *in silico*. **Panel B**. Single-parameter local sensitivity analysis for area under the survival plot. The bars denote mean of 50 runs of sensitivity analyses and error bars the standard errors. Lines denote the 50% sensitivity coefficient threshold. The parameters exceeding this threshold are the fraction of cells removed in surgery (β), death rate (*d*), and division rate (*b*).

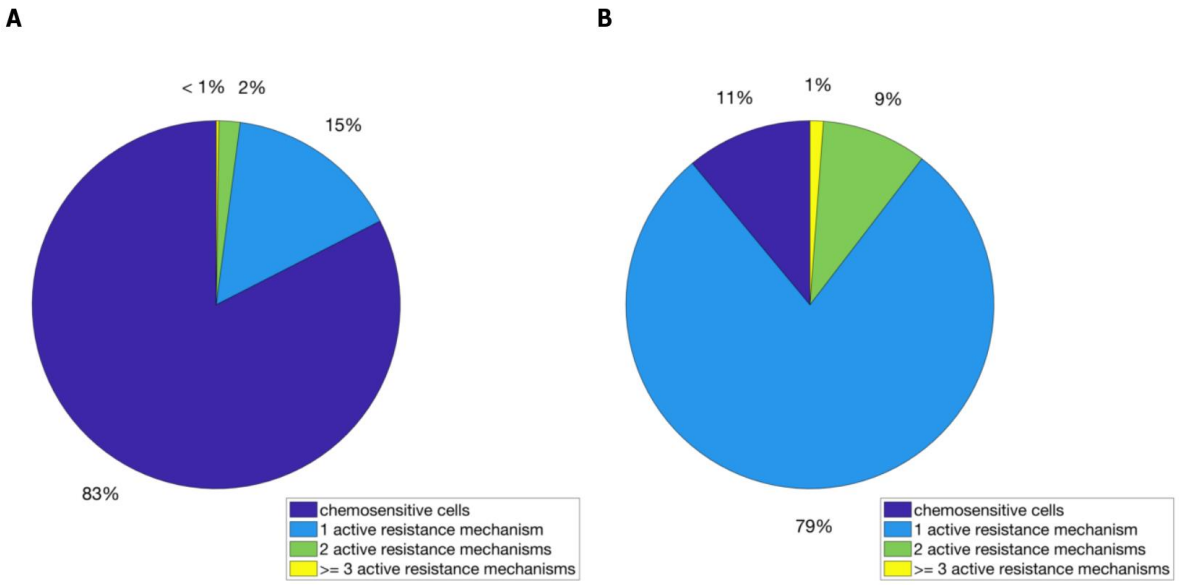

Figure 4. The fraction of active resistance mechanisms before and after neoadjuvant chemotherapy. **Panel A.** Proportion of active resistance mechanisms at diagnosis based on simulation in 1,000 virtual HGSOC patients. **Panel B.** Proportion of active resistance mechanisms after NACT based on simulation in 1,000 virtual HGSOC patients.

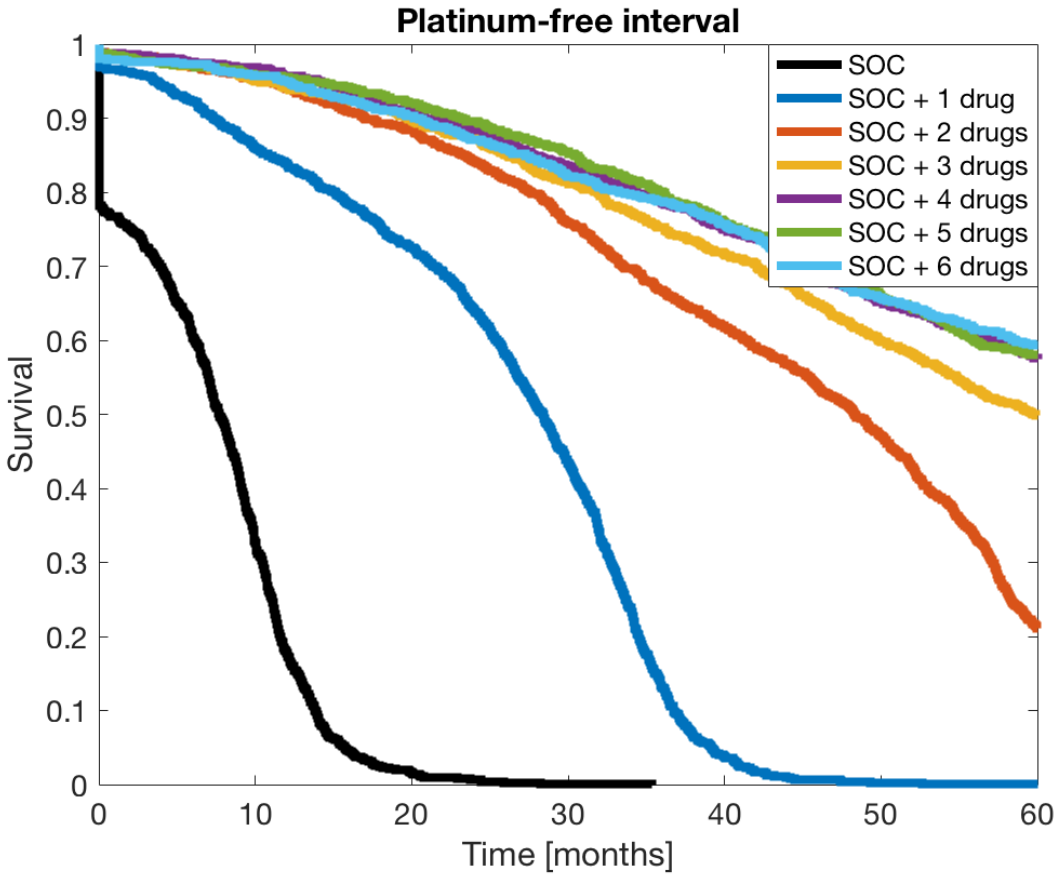

Figure 5. The effect of standard-of-care (SOC) alone or combined with drugs targeting active resistance mechanisms on platinum free interval (PFI). While an average HGSOC patient has five active resistance mechanisms, the tumors are dominated by subpopulations with much fewer active resistance mechanisms. Thus, the use of even one effective targeted therapy in combination with SOC offers a significant survival benefit, whereas adding more than three drugs does not offer a significant further benefit.